Probabilistic seasonal outlook for the rainy season over India by monitoring the onset dates using GPM IMERG satellite-based precipitation

Jayasankar Chempampadam Balasubramannian[1, 2], and Vasubandhu Misra[1, 2, 3]

[1]Center for Ocean-Atmospheric Prediction Studies, Florida State University, Tallahassee, Florida, USA.

[2]Department of Earth, Ocean and Atmospheric Science, Florida State University, Tallahassee, Florida, USA.

[3]Florida Climate Institute, Florida State University, Tallahassee, Florida, USA.

Corresponding Author (Jayasankar Chempampadam Balasubramannian, cbjayasankar@gmail.com)

Abstract

We utilized the Integrated Multi-Satellite Retrievals for Global Precipitation Mission version 6 (IMERG) rainfall observation (available in real time) over India to determine the onset and withdrawal of the rainy season. The annual mean climatology derived from IMERG observations over India aligned closely with the rain gauge-based India Meteorological Department observation. The IMERG rainfall time series was randomly perturbed to generate 101 ensemble members at every grid point of the rainfall analysis to obtain a corresponding ensemble of the onset and withdrawal dates of the rainy season. The perturbations were designed to sample the uncertainty due to random synoptic or mesoscale rain events influencing the diagnosis of the onset/withdrawal dates at the granularity of the IMERG observations (available at 10 km grid). Following earlier studies, we find from the IMERG dataset that seasons with an earlier onset date are strongly related to a lengthier and wetter season, whereas seasons with a later onset date correspond to a shorter and a drier season. In contrast, the connections between ENSO and IOD with the onset, withdrawal, seasonal length, and rainfall of the rainy season were comparatively weaker over most of India. The generation of ensembles in this study underscores the potential for real-time application of generating reliable, probabilistic seasonal outlooks of the rainy season over India by leveraging the local links amongst onset date, seasonal length, and seasonal rainfall anomalies. This potential is further confirmed by the high probabilistic skill scores of the seasonal outlooks using the area under the relative operating characteristic curve method.

1. Introduction

India's water and agriculture sectors rely heavily on copious summer monsoon rainfall, emphasizing its critical role in defining the country's agrarian economy and water resource management (Gadgil and Gadgil 2006). The seasonal progression of the Indian Summer Monsoon (ISM) season has an impact not only on agricultural yields but also on other sectors such as economy and ecology (Lal 2000). Based on rainfall patterns, wind conditions, and outgoing longwave radiation, the India Meteorological Department (IMD) officially declare the date of monsoon onset over Kerala (MoK) each year. In a normal year, the ISM season begins in southern peninsular India on June 1st (with MoK), spreads throughout the country by mid-July, and then begins to retreat on September 1st (Pai et al. 2020).

There are many different definitions for the monsoon onset; however, it is typically considered as a quick, substantial, and prolonged increase in rainfall after May 10th, accompanied by a persistent change in wind direction to southwesterlies associated with the summer monsoon flow (Pai and Rajeevan 2009). In addition to the rainfall-based definitions (e.g., Ananthakrishnan and Soman 1988; Noska and Misra 2016; Misra et al. 2017b), several other atmospheric dynamical and thermodynamical variables (winds, outgoing longwave radiation, temperature, moisture flux convergence, and precipitable water) were utilized to identify the onset of summer monsoon rainfall (e.g., Fasullo and Webster 2003, Zeng and Lu 2004, Prasad and Hayashi 2005, Joseph et al. 2006, Wang et al. 2009, Walker and Bordoni 2016, Stolbova et al. 2016). These variables provide a comprehensive understanding of the atmospheric conditions and dynamics that influence the onset and total summer monsoon rainfall over India. According to Bombardi et al. (2019), monsoon onset detection methods can be grouped into local-scale and regional-to-large-scale approaches, though the latter often show weak correlation with local observations. All these approaches produce somewhat similar onset dates, but their connections with the local-scale onset of the rainfall during the ISM differ (Moron and Robertson 2014; Noska and Misra 2016; Fitzpatrick et al. 2016).

Owing to variations in the onset and withdrawal date of the monsoon season there are considerable spatial and temporal variations in the availability of the rainwater and length of the rainy season

62 (determined solely based on rain rates) over India (Joseph et al. 1994; Lal 2000; Wang et al. 2002;

63 Misra et al. 2017a; Misra et al. 2018). Preenu et al. (2017) indicate from IMD archive that the

64 earliest onset of the ISM was May 11, 1918, and the most delayed onset of ISM was Jun 18, 1972.

65 Several studies discuss the interannual variability of monsoon onset dates in India and its

66 teleconnection with El Niño and the Southern Oscillation (ENSO) and the Indian Ocean Dipole

67 (IOD, Xavier et al. 2007; Sankar et al. 2010; Misra et al. 2017a; Pradhan et al. 2017; Choudhury

68 et al. 2021). In ENSO and IOD years, the monsoon onset is altered by the modulation of the

69 teleconnections with SST anomalies in the tropical oceans, which affect the Walker and Hadley

70 circulations, respectively (Pradhan et al. 2017). Significant changes in the large-scale atmospheric

71 patterns over the monsoon areas are identified during the onset of the monsoon over India (Joseph

72 et al. 1994). According to Wang et al. (2013), the interannual variations in ocean-atmosphere

73 interaction processes significantly influence the association between the monsoon onset and

74 ENSO, which is driven by the meridional SST gradient across the Indian Ocean. Noska and Misra

75 (2016) show that the variations in the onset and withdrawal date of the rainy season over India that

76 largely overlaps with ISM are linked to the variability of the cross-equatorial upper-ocean heat

77 transport in the Indian Ocean, variations in large-scale atmospheric and oceanic circulations, and

78 regional ocean-atmosphere thermal gradients. In addition, internal variability of ISM arising from

79 intraseasonal oscillations (ISOs), can significantly influence the monsoon rainfall and as well as

80 the onset and withdrawal characteristics of the ISM (Goswami and Ajaya Mohan, 2001; Goswami

81 and Xavier, 2005; Karmakar and Misra 2019). Monsoon ISOs are typically classified into active

82 (above normal) and break (below normal) phases, and the frequency of these phases plays a crucial

83 role in determining the seasonal mean monsoon rainfall (Goswami and Ajaya Mohan, 2001).

84 Karmakar and Misra (2019) found that a majority of local onset dates (59%) occur during the

85 positive developing phases of high-frequency ISOs, while a majority of withdrawal dates (62%)

86 occur during the positive decaying phases of low-frequency ISOs.

87

88 It may be noted that we make a subtle distinction between the ISM and rainy seasons, with the

89 latter solely determined by rain rates which includes pre- and post-monsoon seasonal rainfall (e.

90 g., Noska and Misra 2016) while the former is usually a fixed calendar season (June to September)

91 and coincides additionally with the seasonal cycle of circulation features and other thermodynamic

92 factors. Figure S1 highlights the difference between the rainy season and climatological ISM (June

93   to September), which makes it evident that the rainy season accumulates more rainfall in southern
94   peninsular India and in regions east of the central monsoon region. Similarly, when compared to
95   the ISM season, the rainy season has slightly less total rainfall over both western, northern India,
96   and parts of northeastern India. It may be noted that the definition of the rainy season allows for a
97   variable length compared to the fixed calendar season of, which stems from the former including
98   pre-monsoon rainfall and rainfall from pre-monsoon and post-monsoon rainfall. For instance,
99   tropical cyclones are also included in the rainy season defined here, and they significantly
100 contribute to the annual rainfall in some parts of eastern India. Pre- and post-monsoon tropical
101 cyclones can contribute up to 25% of the yearly rainfall in some parts of India, even though the
102 southwest monsoon is the main component of our defined rainy season (Khouakhi et al. 2017).
103
104 The information about the arrival of the monsoon rainfall is imperative for farmers to plan their
105 strategy for the upcoming season. There are many attempts to predict the MoK; however, it
106 remains a challenge due to the intricate interplay between large-scale atmospheric circulation and
107 localized convective processes, resulting in substantial spatial variability in onset dates (Kung and
108 Shariff 1980; Rajeevan and Dubey 1995; Pai and Rajeevan 2007; Pradhan et al. 2017). Many
109 studies have shown that variations of the MoK have very little influence on the mean rainfall
110 anomalies of the ISM (Dhar et al. 1980; Mooley and Parthasarthy 1984; Mooley and Shukla 1987;
111 Misra and DiNapoli 2014). Furthermore, MoK is known to have insignificant relationship with
112 subsequent progression of the onset isochrones of the ISM (Bansod et al. 1991; Fasullo and
113 Webster 2003; Pai and Rajeevan 2007). Noska and Misra (2016) proposed an objective method to
114 define the onset and withdrawal of the rainy season based on area averaged all India daily rainfall,
115 and they found that mean anomalies of the rainy season are closely linked with variations in the
116 onset and withdrawal dates of the rainy season. In addition, they validated the defined onset and
117 withdrawal of the rainy season for consistency by comparing them with the seasonal evolution of
118 key dynamic and thermodynamic variables associated with the ISM. In a following study, Misra
119 et al. (2018) obtained local onset (withdrawal) dates of the Indian rainy season at the granularity
120 of the rainfall analysis and showed that they are negatively (positively) correlated with rainfall
121 anomalies of the rainy season across the Indian region. These studies suggest that monitoring the
122 local onset date of the rainy season provides a good indication of the evolution of the seasonal
123 length and rainfall of the forthcoming rainy season (i.e., the entire duration of the rainy season at

124   each grid points) and supporting its use in predictability studies. Bhardwaj and Misra (2019) found

125   that Remotely Sensed Rainfall Products such as Tropical Rainfall Measuring Mission (TRMM)

126   Multi-satellite Precipitation Analysis (TMPA) produce local onset and withdrawal dates similar to

127   IMD observations. In comparison to traditionally identified onset of ISM, which are often limited

128   to defining the onset over Kerala (e.g., MoK), the proposed method enables the generation of

129   spatially continuous maps of onset date evolution. By capturing regional heterogeneity, it provides

130   a more nuanced understanding of the spatiotemporal progression of onset of the rainy season

131   across India. This simple rainfall-based definition was found useful for monitoring the onset of the

132   rainy season in real-time and issuing the outlook of the rainy season over various regions such as

133   Florida (Misra et al. 2022), and Central America (Rodgers et al. 2024).

134

135   Many studies have used the IMERG data set as one of their primary dataset for the analysis of the

136   ISM (Bushair et al. 2019; Thakur et al. 2020; Saikrishna et al. 2021; Phadtare et al. 2023). In this

137   study, we employ a rainfall-based objective method to define the local onset and withdrawal of the

138   rainy season, leveraging the high-resolution IMERG dataset available since January 2001. Our

139   approach captures the actual arrival and retreat of persistent rainfall at each grid point by

140   identifying the onset and withdrawal of the rainy season. This approach also accounts for pre- and

141   post-monsoon rainfall, providing a more complete representation of the rainy season—particularly

142   in regions where events such as tropical cyclones contribute significantly to seasonal rainfall totals.

143   In this study, utilizing IMERG's 12-hour latency product, we demonstrate the potential for real-

144   time monitoring of the onset of the rainy season, which aids in anticipating the anomalies of the

145   seasonal length and seasonal accumulated rainfall (hereafter referred to as seasonal rainfall) across

146   India. Motivated from the grid-point level definition of onset and withdrawal dates established by

147   Misra et al. (2018) and Bhardwaj and Misra (2019), this study advances this framework by how

148   the IMERG 12-hour latency product can be effectively used to monitor these parameters at fine

149   spatial scales, enabling better anticipation of anomalies of the seasonal length and seasonal rainfall.

150   In addition, the novelty of this work lies in the use of a perturbation technique applied in the

151   diagnosis of onset/withdrawal dates of the rainy season over India following Misra et al. (2023)

152   and Rodgers et al. (2024) to generate 101 ensembles of daily rainfall data. This approach is the

153   first of its kind over the Indian region and allows us to define an ensemble of local onset and

154   withdrawal dates, aiding in the probabilistic estimate of the evolution of the rainy season that

155 accounts for observational and analysis uncertainties. Hereafter, the term 'onset' refers to local or

156 grid point-specific onset dates of the rainy season.

157

158 Additionally, this study explores the interannual variation of the evolution of the rainy season and

159 its link to large-scale forcing such as ENSO and IOD and compares their viability as predictors of

160 the rainy seasons to the local links we establish with the variations of the onset dates. We believe

161 that the insights from this study will have significant potential applications in agricultural planning

162 and water resource management.

163

164 **2. Data and Methodology**

165 **2.1 Data**

166 The analysis performed in this study utilized daily precipitation data from the IMERG version 6

167 (Huffman et al. 2019). This dataset is part of the Global Precipitation Measurement (GPM)

168 mission, which was launched in 2014 and is co-operated by NASA and the Japan Aerospace

169 Exploration Agency (JAXA). The 0.1° grid resolution (~10 km) IMERG data are available at half-

170 hourly intervals from June 2000 to the present. The dataset comprises early, late, and final run

171 products, which have latencies of approximately 4 hours (Early), 12 hours (Late), and 3.5 months

172 (Final). The IMERG late run incorporates data from multiple sources, such as satellite microwave

173 and infrared estimations, precipitation gauge analysis, and other potential precipitation estimators.

174 This dataset provides detailed temporal and spatial coverage for both the TRMM and GPM eras

175 worldwide. However, in this study, we used the daily 12-hour latency product (daily averages were

176 estimated from half-hourly products), which has great potential for monitoring the rainy season in

177 real-time. To assess the fidelity of the 12-hour latency product of IMERG over India, we have

178 compared it with the corresponding Final product of IMERG and also used rain gauge-based IMD

179 gridded rainfall data for the period 2001 - 2023 at 0.25° × 0.25° resolution (Pai et al. 2014) as a

180 validation dataset. Additionally, we defined the onset and withdrawal dates of the rainy season

181 using the daily NOAA Climate Prediction Center (CPC) precipitation data set (Xie et al. 2007)

182 and compared them with IMERG.

183

184 **2.2 Methodology**

185 **2.2.1 Onset and Retreat**

This study uses a simple objective definition to identify the onset and cessation dates of the wet season over India which are determined by finding the minima and maxima of the cumulative rainfall anomaly curve (Liebmann and Marengo 2001). The cumulative anomaly of the daily rainfall at a day J (i.e., $C_i(J)$) for a year i at each grid point is estimated as:

$$C_i(J) = \sum_{j=1}^{J}(R_i(j) - \bar{R}) \qquad (1)$$

where $R_i(j)$ is the rainfall for day j of year i, $\bar{R}$ is the climatology of the annual mean rainfall for a given grid point. The $C_i(J)$ for 365/366 days in a year represents the cumulative rainfall anomaly curve. After the onset and withdrawal dates of the season are determined, we count the number of days between them to define the seasonal length. Seasonal rainfall of the rainy season refers to the daily rainfall that accumulates from the day of onset date to the withdrawal date.

2.2.2 Perturbation

The motivation to perturb the timeseries is to account for the uncertainty of random synoptic or mesoscale events that is potentially unrelated to the seasonal cycle, which could affect the diagnosis of the onset/withdrawal date of the rainy season. The threat of false diagnosis of onset/withdrawal dates of the rainy season is acute from the proposed methodology since this diagnosis is computed at the granularity of the rainfall analysis. Therefore, generating an ensemble of onset/withdrawal dates of the rainy season that accounts for this uncertainty is essential. The perturbations are generated randomly by replacing the rainfall of each day in the original timeseries for a given grid point by rainfall in the range of $\pm$ 3 days. The range of $\pm$ 3 days used in the generation of the perturbed timeseries covers the uncertainty in the occurrence of the synoptic (1 to 7 days) to meso-scale (1 to 3 days) rain features of the rainy season. In this manner, an ensemble of 101 (100 perturbations + 1 original) timeseries are generated. The diagnosis of the onset/withdrawal date of the rainy season will converge or diverge amongst the ensemble members if it is found to be insensitive or sensitive to these random rain events, respectively.

2.2.3 Signal-to-noise Ratio

We estimated the signal-to-noise ratio of the four quantities by utilizing the 101 ensemble members.

217 $$S_{noise}^2 = \frac{1}{A(B-1)} \sum_{a=1}^{A} \sum_{b=1}^{B} (X_{ab} - \bar{X}_b)^2 \qquad (2)$$

218 $$S_{signal}^2 = S_{em}^2 - \frac{1}{b} S_{noise}^2 \qquad (3)$$

219 Where, X belongs to any of the four quantities such as onset date, withdrawal date, seasonal length,

220 and seasonal rainfall anomalies of the varying rainy season, a and b are indices for A years and B

221 ensemble members, respectively. S_{em}^2 represents the measured total signal variance in the data over

222 A years and which is defined as;

223 $$S_{em}^2 = \frac{1}{(A-1)} \sum_{a=1}^{A} (\bar{X}_a - \bar{\bar{X}})^2,$$

224 And $\bar{X}_a = \frac{1}{(B-1)} \sum_{b=1}^{B} X_{ab}$, $\bar{\bar{X}} = \frac{1}{(A-1)} \sum_{a=1}^{A} \bar{X}_a$,

225 The signal-to-noise ratio is then given by:

226 $$ratio = \frac{S_{signal}^2}{S_{noise}^2} \qquad (4)$$

227 When $ratio < 1$ then it indicates that noise (or chaotic variations) is dominant, and the signal

228 dominates when $ratio > 1$. A strong signal indicates that perturbing the rainfall time series will

229 not substantially influence the diagnostics of the onset date, withdrawal date, seasonal length, and

230 seasonal rainfall anomalies.

231

232 **2.2.4 Significance test**

233 In this study, we first estimate the two-tailed p-values of the correlation coefficients using the t-

234 statistic. Further, following Benjamini and Hochberg (1995), we conduct a test for false rejection

235 on all temporal correlations to assess its robustness, which is necessary because of the large number

236 of simultaneous statistical significance tests conducted across all grid points of the domain. This

237 process involves adjusting the p-value (Benjamini and Hochberg 1995) to control the false

238 rejection of the null hypothesis, also known as the false discovery rate. By controlling the false

239 discovery rate, we enhance the confidence in the significance of the findings.

240

241 **3. Results**

242   The seasonal mean rainfall over India observed from IMERG is found to be comparable with IMD
243   observation and superior to other satellite products over the region (Saikrishna et al., 2021). This
244   is further confirmed in Figs. 1a-c which compares the 23-year annual mean rainfall climatology
245   between IMERG observations and the corresponding IMD rainfall dataset. It may be noted that in
246   Equation (1), the annual mean rainfall climatology ($\bar{R}$) at each grid point is used to determine
247   onset dates and withdrawal dates of the rainy season over India (e.g., Misra et al., 2018). Overall,
248   the annual mean rainfall climatology from IMERG compares well with the IMD rain gauge dataset.
249   However, the overestimation of rainfall in the Indo-Gangetic plains and parts of northeast India
250   and underestimation of rainfall over the northern Western Ghats, northern sections of northeast
251   India, and the bulk of Jammu and Kashmir by IMERG relative to IMD dataset is apparent (Fig. 1).
252   Bushair et al., (2019) noted that IMERG underestimates the rainfall over high-altitude regions
253   compared to IMD observations, which are rain gauge based. Further, Fig. 1d shows the cumulative
254   rainfall anomaly curve generated from the 23-year (2001 - 2023) daily rainfall climatology area
255   averaged over all of India for IMERG (blue) and IMD (red) observations. The onset (inflection at
256   the nadir of the cumulative anomaly curve) and withdrawal (inflection at the zenith of the
257   cumulative anomaly curve) dates estimated from IMERG and IMD closely match each other, with
258   the onset dates being 31st May and 3rd June, and the withdrawal dates being 7th October and 8th
259   October, respectively.
260

261
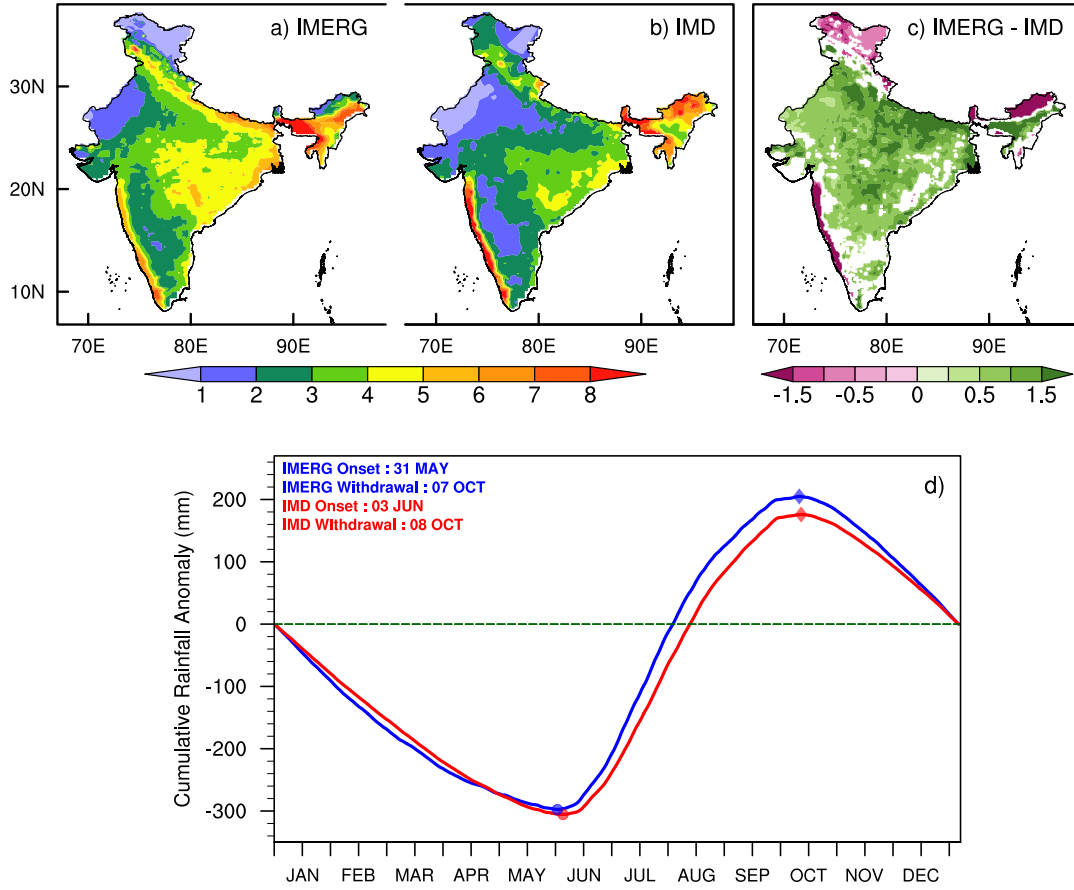
Figure 1: *Spatial pattern of the 23-year climatology of the mean annual rainfall (mm/day) during the period 2001-2023 from a) IMERG observation, b) IMD observation, and c) the difference between the IMERG and IMD (only differences significant at 5% percentile level on t-test is shaded). d) The cumulative rainfall anomaly curve generated from the 23-year daily rainfall climatology of IMERG (blue) and IMD (red) observations. The onset dates (filled circles) and withdrawal dates (filled diamonds) obtained from both datasets are marked.*

268

Figures 2a-d depict the 23-year local climatological onset date, withdrawal date, seasonal length, and seasonal accumulated rainfall from IMERG, with the associated standard deviation displayed in Figs. 2e-h. The spatial distribution of the climatology of the onset dates (Fig. 2a) shows the earliest onset occurs over northeast regions of India followed by southern Kerala, and then it gradually advances to the other parts of the country and looks like the typical isochrone evolution of the ISM (Ramage 1971; Rao 1976; Janowiak and Xie 2003). The delayed onset occurs over the east coast of Tamil Nadu followed by Jammu and Kashmir. The onset dates over Kerala and

276 adjacent regions mostly start from early May and do not coincide with the MoK, and this is because
277 this methodology detects the onset dates relatively early due to strong and continuous spells of
278 pre-monsoon rainfall. Similarly, the earliest withdrawal (Fig. 2b) of the ISM occurs over
279 northwestern India such as Rajasthan, Punjab, Haryana, and Himachal Pradesh. The withdrawal
280 date is delayed over southern peninsular India, with the most delayed withdrawal occurring over
281 the southeast coast of Tamil Nadu. The seasonal length (Fig. 2c) is shorter in the west and
282 northwest regions of India, with the shortest season in Jammu and Kashmir. The longer season
283 over the peninsular India, as well as the coastal regions of Odisha and West Bengal, is linked to
284 the season's earlier start date. The spatial distribution of the seasonal accumulated rainfall (Fig.
285 2d) closely follows the typical seasonal mean ISM distribution. The standard deviation patterns of
286 the onset dates show central parts of India have less variability than other regions, such as southern
287 peninsular India, northeast, and northwest regions. Similar patterns of variability are observed in
288 the withdrawal dates and seasonal length with the largest variations found over southern peninsular
289 India and northwest India and least over central India. On the other hand, the seasonal rainfall
290 exhibits a significant range of variability across most of India, whereas comparatively less
291 variability is observed over Rajasthan and Jammu and Kashmir.

292
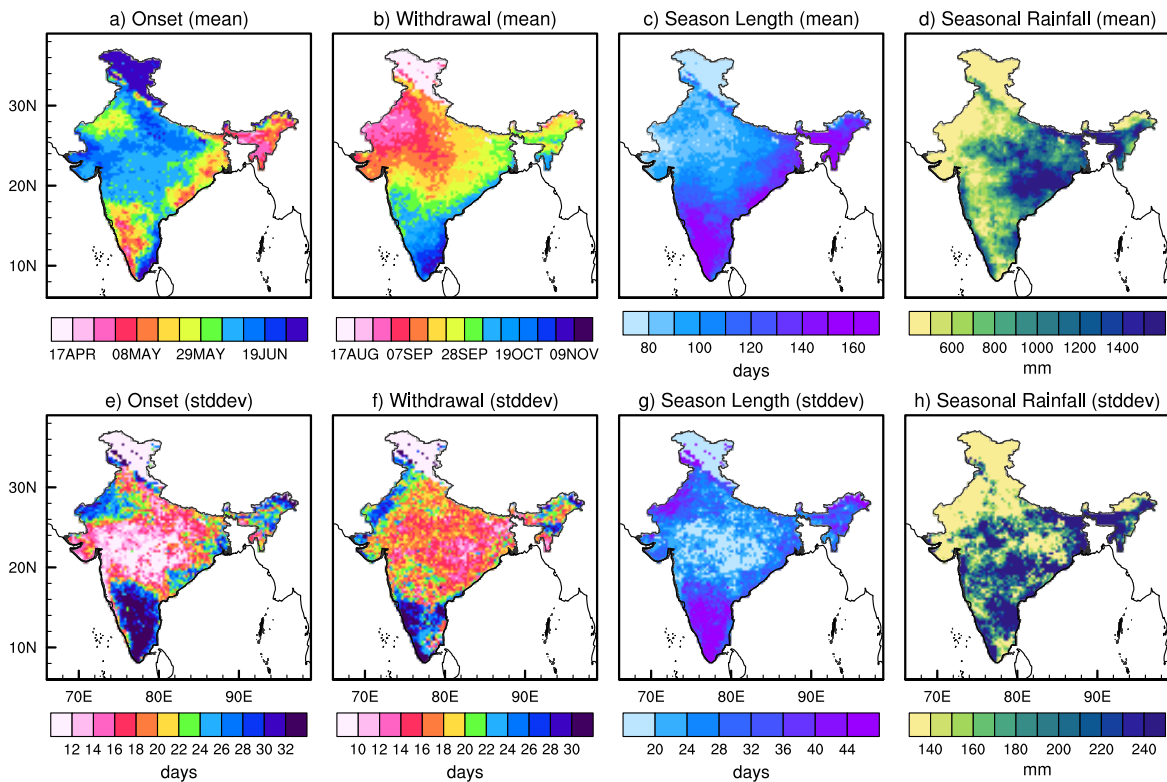
293 ***Figure 2****: The climatological a) onset date (Julian day), b) withdrawal date (Julian day), c)*
294 *seasonal length, and d) seasonal accumulated rainfall (mm) of the rainy season from IMERG. The*
295 *corresponding standard deviation of e) onset date (days), f) withdrawal date (days), g) seasonal*
296 *length (days), and h) seasonal accumulated rainfall (mm). The contour intervals in panels (a) and*
297 *(b) are at 7-day interval.*
298

299 The IMERG dataset, with its 23-year record, was compared to the IMD and CPC datasets spanning
300 1979–2023 (limited to this period in order for CPC and IMD to have a common period) to evaluate
301 onset and withdrawal dates, seasonal length, and seasonal accumulated rainfall of the rainy season
302 over India (Fig. S2). The motivation to carry out this comparison is to establish that a 23-year
303 record of IMERG is comparable to a longer record of dataset available from the other two sources
304 besides examining its fidelity.
305

306 It is apparent from Fig. S2 that the spatial patterns of the climatological onset and withdrawal
307 dates, seasonal length, and rainfall in IMERG is comparable to corresponding climatologies from
308 IMD and CPC datasets. There is however a tendency for IMERG to have a bias of a slightly earlier
309 onset of the rainy season compared to IMD and CPC, particularly over southern peninsular India,
310 including Kerala and Tamil Nadu (Figs. S2a-c). Similar inference can be drawn in Rajasthan,
311 coastal Odisha and West Bengal, and few isolated grid points over other regions. In contrast, over
312 Jammu and Kashmir, IMERG exhibits a noticeably delayed onset, which makes us unsure about
313 the results over this area. Similarly, IMERG display a systematic bias of slightly later withdrawal
314 dates along the Western Ghats, but overall, the rainy season withdrawal dates are consistent across
315 datasets (Figs. S2e-g). As a result, IMERG's rainy season seems to last longer than the other two
316 datasets in some of these locations (Figs. S2i-k). Again, in terms of seasonal accumulated rainfall
317 (Figs. S2m-o), IMERG overestimates precipitation compared to IMD and CPC in some of these
318 locations. However, rainfall over the Western Ghats exhibits stronger gradients and is
319 underestimated in IMERG while it exhibits more rainfall over western central India and Tamil
320 Nadu than the other two datasets.
321

322 The interannual variability of these variables in IMERG also appear to be comparable to the other
323 two datasets, especially in their spatial gradients (Fig. S3). There are however instances of some

324   differences in the datasets. For example, over central India, the standard deviation of seasonal
325   rainfall is significantly overestimated in IMERG compared to IMD (Figs. S3m-o), even though
326   the withdrawal dates (Figs. S3e-g) and seasonal length (Figs. S3i-k) exhibit less variability in
327   IMERG.

328

329   As mentioned earlier, IMERG has few different rainfall products based on the latency of their
330   availability in real-time. We have made comparisons of 12-hour latency product with the Final
331   product of IMERG in Figs. S1, S2, and S3. The comparison in Fig. S1 indicates that some of the
332   largest differences in the seasonal rain of the variable rainy season between Final and 12-hour
333   latency of IMERG is over northern India. However, the spatial patterns of the climatological onset
334   appear comparable (Figs. S2c and d). But the climatological withdrawal dates appear to be slightly
335   earlier in northern India in the Final run (Fig. S2h) compared to 12-hour latency (Fig. S2g) of
336   IMERG, which likely leads to slightly shorter length (Fig. S2l) and reduced seasonal rainfall (Fig.
337   S2p) in the former (Fig. S2l) than in the latter (Figs. S2k and o). Some of the discrepancies
338   observed in the 12 hour latency product of IMERG relative to IMD and CPC in Figs. S2 and S3
339   can likely be attributed to the uncertainty associated with the choice of the 12-hour latency product,
340   which is an early version of IMERG with limited calibration against ground-based observations,
341   its shorter temporal coverage of 23 years compared to the 45 years of data used for IMD and CPC.
342   Despite these limitations, which seem to be tolerable for the applications of this study (compare
343   Fig. 1) we are inclined to use IMERG due to its higher spatial resolution and near real-time
344   availability making it particularly suitable for real-time applications.

345

346   The primary motivation to monitor the local onset and withdrawal of the ISM is its significant
347   interannual variations and spatial variability (Fig. S3). Both the variation in seasonal length and
348   seasonal rainfall are crucial in determining the nature of the rainy season (Xavier et al.
349   2007; Sperber and Annamalai 2014). The spatial distribution of the correlation of the local onset
350   date with the seasonal length shows a significant negative correlation across India except in some
351   parts of central India and Jammu and Kashmir (Fig. 3a). This negative correlation suggests that an
352   early or later onset date is likely to be associated with a longer or a shorter rainy season,
353   respectively. Only the correlations significant at a 5% level are shaded (non-significant values are
354   shown in white) in Fig. 3. Similarly, early onset is associated with a wetter season, while a delayed

355   onset is linked with a drier season (Fig. 3b). However, the grid points showing significant

356   correlation are fewer in Fig. 3b compared to Fig. 3a. The correlations of the withdrawal date with

357   seasonal length (Fig. 3c) and seasonal rainfall anomalies (Fig. 3d) show that later or early

358   withdrawal of the wet season corresponds to a longer and wetter season, whereas an earlier

359   withdrawal corresponds to shorter and drier seasons. While the correlation between seasonal

360   rainfall and onset/withdrawal dates appears weaker than that with seasonal length, over 50% of

361   grid points across India still show statistically significant relationships. This is expected, as total

362   rainfall during the rainy season is influenced by variations in the seasonal length but also daily rain

363   rate, which can be influenced by various factors like tropical cyclones and intraseasonal weather

364   patterns that may lead to a weak correlation with onset/withdrawal dates. However, the withdrawal

365   date may not be a useful predictor for the rainy season because it occurs when the rainy season

366   ends. The onset and withdrawal dates are largely uncorrelated (not shown), implying that their

367   variations are independent of each other. These outcomes imply that the onset date alone can be a

368   useful predictor for the outlook of the seasonal length and the seasonal rainfall anomaly of the

369   forthcoming rainy season.

370
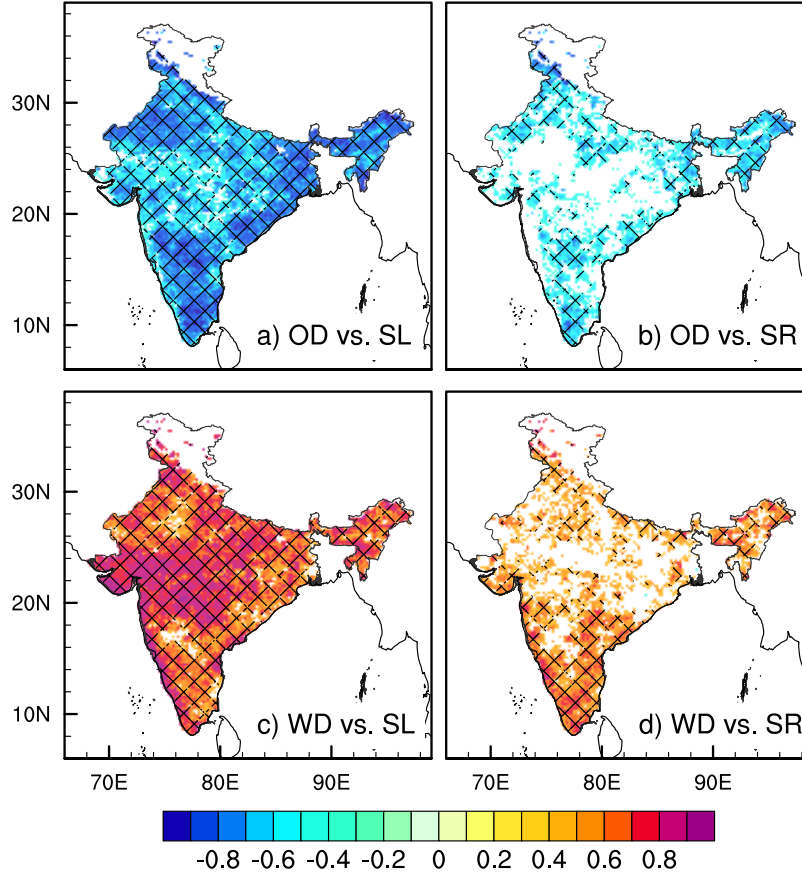
Figure 3: *The correlation coefficients of the onset date (OD) with a) seasonal length (SL), and b) seasonal rain (SR). Similarly, the correlations of withdrawal date (WD) with c) SL and d) SR. The shading indicates statistical significance at a 5% significance level according to the t-statistic (non-significant values are shown in white), following false discovery rate testing as described by Benjamini and Hochberg (1995). Cross hatchings denote correlations greater than or equal to +/- 0.6.*

We estimated the signal-to-noise ratio (Equation 4) on the four variables of onset and withdrawal dates, seasonal length, and rainfall by utilizing the 101-member ensemble of time-series data. This analysis examines the spread across ensemble members and informs on the uncertainty of the diagnosis to random rain events. The signal-to-noise ratio for onset dates (Fig. 4a) shows that noise dominates in many places, particularly in peninsular India and the eastern half of central India. These low signal-to-noise ratio regions suggests that onset dates of the rainy season are not very strongly tied to the seasonal cycle and predicting the onset dates in these places becomes challenging and less reliable. In contrast, the signal-to-noise ratios for withdrawal dates (Fig. 4b)

387 are typically more than one over most grid points. This indicates greater certainty for withdrawal
388 dates, particularly in areas like Kerala, coastal Karnataka, and Gujarat, where the ratios are
389 comparatively higher than one. In the case of the seasonal length, signal dominates over noise with
390 a signal-to-noise ratio above 1 over most areas (Fig. 4c). Compared to the other variables, seasonal
391 rainfall generally shows much higher signal-to-noise ratios (> 1) across most of the grid points.
392 This result is obvious given the fact that seasonal rainfall is an aggregate of the daily rainfall over
393 the entire rainy season, while the onset and withdrawal dates are single days of the season when
394 they are diagnosed. Therefore, there is a tendency for the cancellation of the noise in the
395 aggregation of the daily rainfall to seasonal rainfall, which yields a higher signal-to-noise ratio.

396
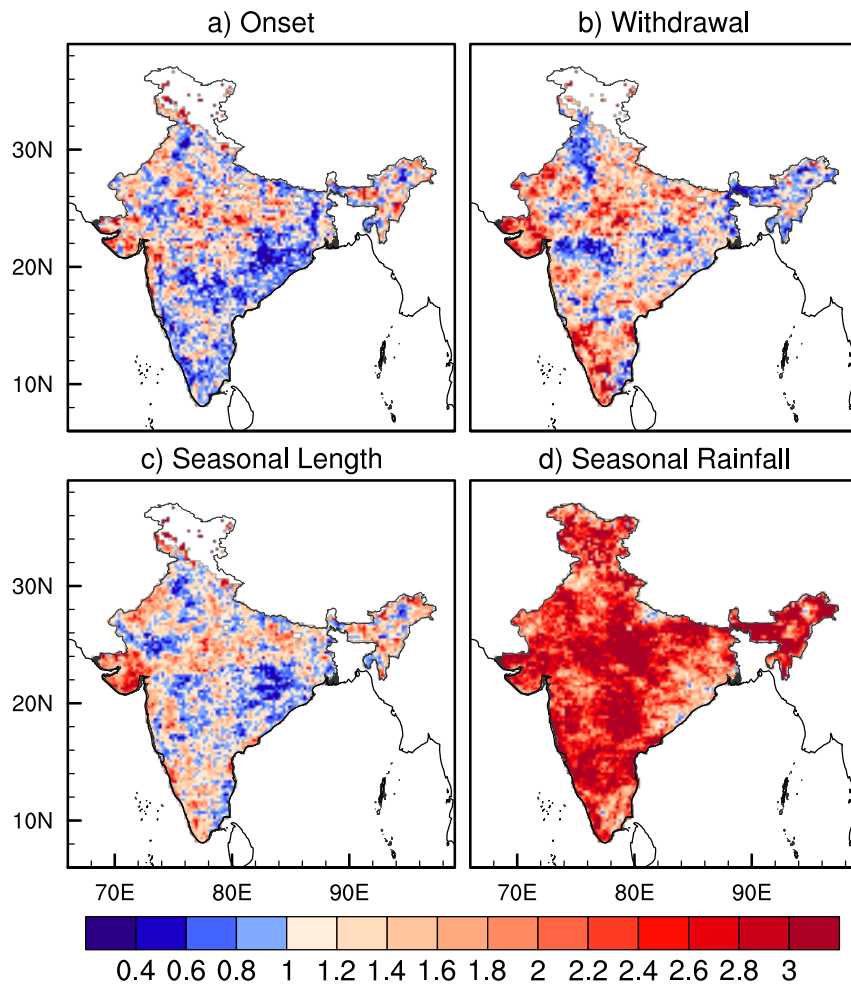
397 ***Figure 4****: The 23-year climatology of the signal-to-noise ratio of a) onset date, b) withdrawal date,*
398 *c) seasonal length, and d) seasonal rainfall estimated based on the 101 ensemble members.*

Further, we examined the probabilistic skill of the seasonal outlook by using the Area Under the relative operating characteristic (ROC) Curve (AUC) method. The AUC method is widely used to assess the skill of seasonal climate predictions (Mason and Graham 2002; Misra 2004; Narotsky and Misra 2021). Previous studies have shown that this method is useful for evaluating the probabilistic skill of predicting anomalous seasons based on anomalous onset dates of the rainy season (e.g. Rodgers et al 2024). We categorized the onset date, seasonal length, and seasonal rainfall into terciles (23-years divided into three groups): the lower tercile represents an early onset, shorter season, and drier conditions; the upper tercile signifies a delayed onset, longer season, and wetter conditions; and the middle tercile indicates normal onset, length, and seasonal rainfall. We then created a contingency table (Table S1) to assess the probability of categorical forecasts. This table evaluates how often an early or late onset is linked with a shorter or longer season and with drier or wetter conditions, respectively. In addition, we also consider the effects of normal onset on normal length and seasonal rainfall.
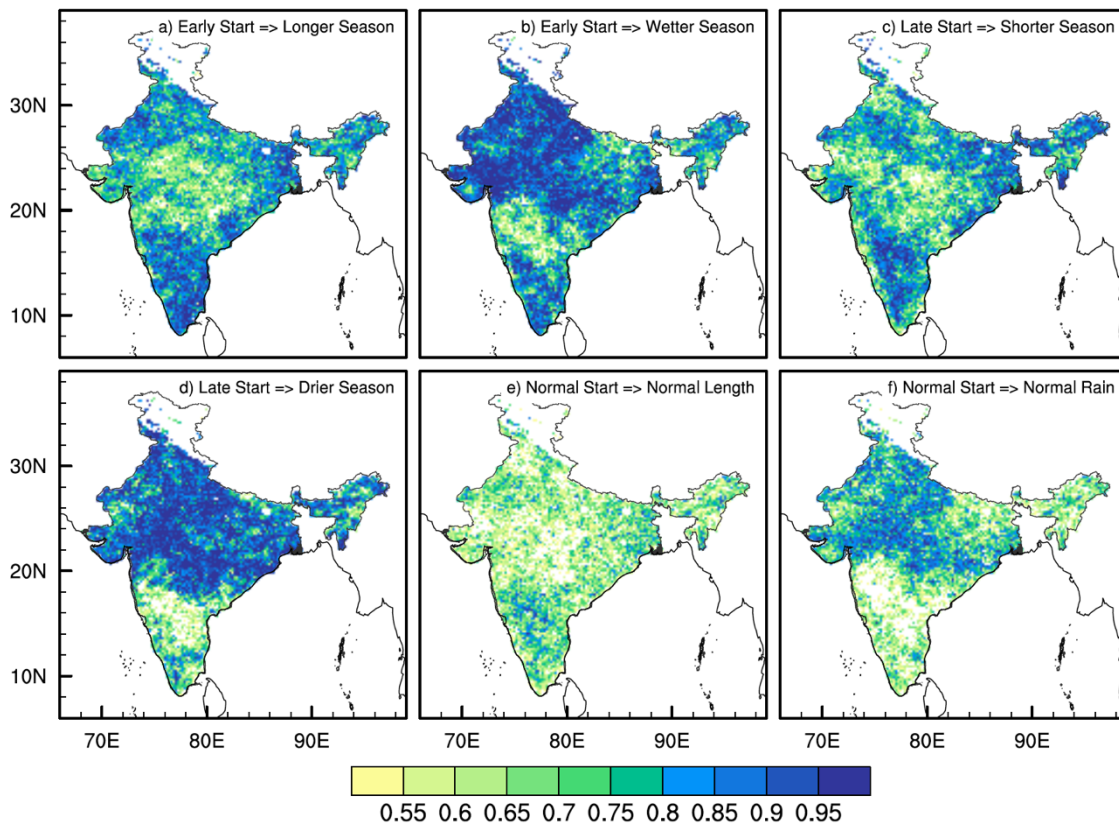
Figure 5: *The probabilistic skill score as measured by the Area Under the relative operating characteristic Curve (AUC) for early start (lowest tercile) season associated with a) longer*

415   *(highest tercile) and b) wetter (highest tercile) season, late start (highest tercile) season associated*

416   *with c) shorter (lowest tercile) and d) drier (lowest tercile) season, and normal (middle tercile)*

417   *start season associated with e) normal (middle tercile) seasonal length and f) normal (middle*

418   *tercile) seasonal rain. The AUC above 0.5 is shaded.*

419

420   The probabilistic skill scores derived from the AUC method are shown in Fig. 5. Here, only grid

421   points with AUC values ≥ 0.5 are shaded, as these points indicate skillful seasonal outlooks that

422   outperform random predictions (Mason and Graham, 2002). The seasons with an early start and

423   longer season (Fig. 5a) show the most skill (>0.9) over peninsular India, northwest India, and some

424   parts of northeast India. Similarly, the early start of the season, along with the wetter season (Fig.

425   5b), results in high skill levels across most parts of India except the majority of Maharashtra and

426   north interior Karnataka. The late start and associated shorter seasons shown in Fig. 5c exhibit the

427   highest skill score over some parts of peninsular India. The late start with the drier season also

428   resulted in high skill scores across most of the areas except Kerala, Tamil Nadu, Karnataka and

429   Andhra Pradesh. The anomalous seasons (Fig. 5a-d) demonstrate higher skill levels across India

430   compared to the normal seasons (Fig. 5e-f). This is due to the leveraging of the linear relationships

431   of the onset date variations with the rainy season variations (Figs. 3a and b). In contrast, seasons

432   with a normal start of the rainy season exhibit lower AUC skill scores (Figs. 5e and f) across most

433   grid points relative to the anomalous start of the rainy seasons (Figs. 5a-d). However, the skill

434   scores for a normal start with normal rainfall (Fig. 5f) are slightly better than those for a normal

435   start with normal length (Fig. 5e). In summary, the behavior of the forthcoming season is more

436   predictable if the onset date is early or delayed than the normal. It is easy to adopt this methodology

437   for real-time applications. The evolution of the daily cumulative anomaly curve of rainfall could

438   be monitored in real-time to find the minima in the curve as the onset date. However, to avoid

439   misdiagnosing the onset date of the rainy season, one could wait for a period of time after this

440   diagnosis (typically a week) to confirm that the minima were indeed reached to declare the onset

441   date. Once the onset date is diagnosed then one could use the linear relationships shown in Fig. 3

442   to develop a seasonal outlook for the rainy season. This is done routinely in Florida (Misra et al.

443   2022). With the availability of the merged IMERG estimates with the rain-gauge based IMD

444   rainfall following Mitra et al., (2009) our proposed methodology could be adopted for real-time

445   applications over India.

446

447   Further, we investigated the interannual variability of the onset dates over India and its association

448   with ENSO (Figure S4) and the Indian Ocean Dipole (IOD) variations (Figure S5). In comparison

449   to Figure 3, Figures S4 and S5 failed the BH test suggesting the lack of robustness in the

450   teleconnections of the rainy season variations with either ENSO or IOD. It should be noted that

451   the results in Figures S4 and S4 appear to be contrary to many other studies that suggest a robust

452   teleconnection of ENSO with ISM (e. g., Webster et al. 1998, Delsole and Shukla 2002). However,

453   our variable definition of the rainy season which includes pre- and post-monsoon rainfall would

454   make the comparison with other studies dealing with fixed calendar ISM season and or all India

455   averaged rainfall of the ISM incompatible. But in light of these results that indicate a lack of strong

456   external forcing, the significance of the reliability of the seasonal outlook of the rainy season

457   shown in Figure 5 assumes greater significance. Furthermore, the monitoring of the observations

458   of the evolution of the rainy season to diagnose the onset dates seems an attractive approach with

459   the relatively low signal-to-noise ratio of the onset date of the rainy season shown in Figure 4a

460   relative to the seasonal length in Figure 4c or seasonal rainfall in Figure 4d. We are then able to

461   leverage a low signal-to-noise ratio quantity like the onset date of the rainy season to provide a

462   seasonal outlook of relatively higher signal-to-noise ratio quantities of seasonal length and rainfall.

463

464   **4.   Summary and Concluding Remarks**

465   The seasonal prediction of the Indian rainy season is a considerable challenge given its complex

466   spatio-temporal variations. In this study, we offer a simple and reliable technique for seasonal

467   outlook of the rainy season, which is viable for real-time applications as well. Using precipitation

468   estimates of IMERG version 6 over India at 10km grid, we generate an ensemble of 101 members

469   from randomly perturbing the series to assess the uncertainty of the diagnosed onset/withdrawal

470   dates of the rainy season to random synoptic-meso scale rain events unconnected to the seasonal

471   cycle. The proposed method generates a spatial distribution of local-scale onset and withdrawal

472   dates, capturing regional variations and offering a nuanced view of progression rainy season across

473   India. Such location-specific information is useful for practical applications such as agriculture,

474   disaster planning, and water management.

475

476   We verified the IMERG rainfall observations against gauge-based IMD observations. The mean
477   annual rainfall climatology of IMERG closely matches that of the IMD. However, IMERG tends
478   to underestimate mean annual rainfall in high-altitude regions and overestimate it in the Indo-
479   Gangetic plains. Further, we examined the relationships between the onset and withdrawal dates
480   with seasonal length and rainfall and discovered that variations in onset and withdrawal dates of
481   the rainy season across India have a significant impact on the seasonal length and the seasonal
482   rainfall variations of the rainy season. It is found that an earlier onset date of the rainy season is
483   strongly related to a longer and wetter season, whereas a later onset date corresponds to a shorter
484   and drier season. However, the relationship between the onset, withdrawal, seasonal length, and
485   rainfall with large-scale climate drivers such as ENSO and IOD is comparatively weaker in major
486   parts of India. Although the influence of ENSO and IOD were investigated in this study, future
487   research could investigate the influence of additional teleconnection patterns such as the Madden–
488   Julian Oscillation (MJO), Pacific Decadal Oscillation (PDO), and North Atlantic Oscillation
489   (NAO), which may also modulate the timing and characteristics of the rainy season.
490
491   This study shows that by estimating the onset date of the rainy season alone we can effectively
492   provide a reliable seasonal outlook for both the seasonal length and total rainfall of the upcoming
493   season by exploiting the existing local relationships. The low signal to noise ratio of the onset date
494   of the rainy season suggests the dominance of internal variations, which will be a challenge for its
495   seasonal predictability. However, by way of monitoring the evolution of the onset date we can
496   leverage its local relationship with the length and seasonal rainfall anomaly to provide reliable
497   seasonal outlook of the rainy season. The probabilistic skill scores of these seasonal outlooks
498   generated from the monitoring of the onset date variations present an objective measure of its high
499   confidence of reliability. Compared to traditional ISM onset definitions, which often focus on
500   Kerala (e.g., MoK), the proposed method can generate spatial maps of local-scale onset dates of
501   the rainy season. It captures regional heterogeneity and the progression of the rainy season across
502   India. Since the method is based on the rainy season and includes pre- and post-monsoon rainfall,
503   it provides a comprehensive viewpoint of the rainy season. These seasonal outlooks have
504   numerous potential applications, and many local communities could greatly benefit from them.
505   The proposed methodology for the seasonal outlook of the rainy season over India demonstrates

506   its adaptation for real-time applications from the current availability of IMERG rainfall products

507   in real-time.

508

509   **Acknowledgments**

510   We acknowledge the support from NASA grant 80NSSC22K0595.

511

512   **Code/Data Availability**

513   The IMERG rainfall dataset is available from the NASA GES DISC

514   (https://gpm1.gesdisc.eosdis.nasa.gov/data/GPM_L3/GPM_3IMERGDL.06/). The India

515   Meteorological Department rainfall data set used for the analysis in this study is available at

516   https://www.imdpune.gov.in/cmpg/Griddata/Rainfall_25_NetCDF.html. The daily CPC data is

517   obtained from https://psl.noaa.gov/data/gridded/data.cpc.globalprecip.html. The Python and NCL

518   codes used for the analysis can be provided by the corresponding authors upon request.

519

520   **Author contribution**

521   The study was conceptualized by CBJ and VM. CBJ carried out the analysis and validation and

522   prepared the original manuscript. VM supervised the work, acquired funding, and reviewed and

523   edited the manuscript.

524

525   **Competing interests**

526   The authors declare that they have no conflict of interest.

527

528   **Reference:**

529   1.   Ananthakrishnan, R., and M. K. Soman, (1988). The onset of the southwest monsoon over

530   Kerala: 1901–1980. J. Climatol., **8**, 283–296, doi:10.1002/joc.3370080305.

531   2.   Bansod, S. D., S. V. Singh, and R. H. Kripalani, 1991: The relationship of monsoon onset

532   with   subsequent   rainfall   over   India. *Int.   J.   Climatol.*, **11**, 809–817,

533   doi:10.1002/joc.3370110707.

534   3.   Benjamini, Y., & Hochberg, Y. (1995). Controlling the false discovery rate: A practical and

535   powerful approach to multiple testing. Journal of the Royal Statistical Society: Series

536   B, 57(1), 289–300. https://doi.org/10.1111/j.2517-6161.1995.tb02031.x

4. Bhardwaj, A., & Misra, V. (2019). Monitoring the Indian summer monsoon evolution at the granularity of the Indian meteorological sub-divisions using remotely sensed rainfall products. Remote Sensing, 11(9), 1080. https://doi.org/10.3390/rs11091080

5. Bombardi, R. J., Moron, V., & Goodnight, J. S. (2020). Detection, variability, and predictability of monsoon onset and withdrawal dates: A review. Int. J. Climatol, 40(2), 641-667. https://doi.org/10.1002/joc.6264

6. Bushair, M. T., Kumar, P., & Gairola, R. M. (2019). Evaluation and assimilation of various satellite-derived rainfall products over India. International Journal of Remote Sensing, 1–24. https://doi.org/10.1080/01431161.2019.1579389

7. Choudhury, D., Nath, D., & Chen, W. (2021). The modulation of Indian summer monsoon onset processes during ENSO through equatorward migration of the subtropical jet stream. Climate Dynamics, 57(1), 141-152. https://doi.org/10.1007/s00382-021-05700-4.

8. Delsole, T, and J. Shukla, (2002). Linear prediction of Indian Monsoon Rainfall. J. Climate, 15, 3645-3658. https://doi.org/10.1175/1520-0442(2002)015<3645;LPOIMR>2.0.CO;2

9. Dhar, O. N., P. R. Rakhecha, and B. N. Mandal (1980), Does the early or late onset of monsoon provide any clue to subsequent rainfall during the monsoon season, Mon. Weather Rev., 108, 1069–1072, doi:10.1175/1520-0493(1980)1082.0.CO;2

10. Fasullo J, Webster PJ (2003) A hydrological definition of Indian monsoon onset and withdrawal. J Climate 16:3200–321. https://doi.org/10.1175/1520-0442(2003)016<3200a:AHDOIM>2.0.CO;2

11. Fitzpatrick, R. G., Parker, D. J., & Willetts, P. D. (2016). Assessing the level of spatial homogeneity of the agronomic Indian monsoon onset. Geophysical Research Letters, 43(22), 11-867. https://doi.org/10.1002/2016GL070711

12. Gadgil, S.; Gadgil, S (2006). The Indian Monsoon, GDP and Agriculture. Econ. Polit. Wkly. 41, 4887–4895. https://www.jstor.org/stable/4418949

13. Goswami, B. N., & Mohan, R. A. (2001). Intraseasonal oscillations and interannual variability of the Indian summer monsoon. Journal of climate, 14(6), 1180-1198. https://doi.org/10.1175/1520-0442(2001)014<1180:IOAIVO>2.0.CO;2

14. Goswami, B. N., & Xavier, P. K. (2005). ENSO control on the south Asian monsoon through the length of the rainy season. *Geophysical Research Letters*, *32*(18). https://doi.org/10.1029/2005GL023216

568   15. Huffman, G. J., Bolvin, D. T., Braithwaite, D., Hsu, K. L., Joyce, R. J., Kidd, C., ... & Xie,
569   P. (2020). Integrated multi-satellite retrievals for the global precipitation measurement
570   (GPM) mission (IMERG). In *Satellite precipitation measurement: Volume 1* (pp. 343-353).
571   Cham: Springer International Publishing. https://doi.org/10.1007/978-3-030-24568-9_19

572   16. Janowiak, J. E., and P. Xie (2003), A global-scale examination of monsoon-related
573   precipitation, J. Clim., 16, 4121–4133. https://doi.org/10.1175/1520-
574   0442(2003)016<4121:AGEOMP>2.0.CO;2

575   17. Joseph PV, Eishcheid JK, Pyle RJ. (1994). Interannual variability of the onset of the Indian
576   summer monsoon and its association with atmospheric features, El Nino, and sea surface
577   temperature anomalies. Journal of Climate 7: 81–105. https://doi.org/10.1175/1520-
578   0442(1994)007<0081:IVOTOO>2.0.CO;2

579   18. Joseph PV, Sooraj KP, Rajan CK (2006). The summer monsoon onset process over South
580   Asia and an objective method for the date of monsoon onset over Kerala. Int J Climatol
581   26:1871–1893. https://doi.org/10.1002/joc.1340

582   19. Karmakar, N., & Misra, V. (2019). The relation of intraseasonal variations with local onset
583   and demise of the Indian summer monsoon. *Journal of Geophysical Research:*
584   *Atmospheres*, *124*(5), 2483-2506. https://doi.org/10.1029/2018JD029642

585   20. Khouakhi, A., Villarini, G., & Vecchi, G. A. (2017). Contribution of tropical cyclones to
586   rainfall at the global scale. Journal of Climate, 30(1), 359-372.
587   https://doi.org/10.1175/JCLI-D-16-0298.1

588   21. Kung, E. C., and Sharif, T. A., (1980). Regression forecasting of the onset of the India
589   summer monsoon with antecedent upper air conditions, J. Appl. Meteorol., V19, pp370—
590   380. https://doi.org/10.1175/1520-0450(1980)019<0370:RFOTOO>2.0.CO;2

591   22. Lal, M. (2000). Climatic change-implications for India's water resources. Journal of Social
592   and Economic Development, 3, 57-87. https://ideas.repec.org/a/sch/journl/v3y2001i1p57-
593   87.html

594   23. Liebmann, B., and J. Marengo, (2001). Interannual variability of the rainy season and
595   rainfall in the Brazilian Amazon basin. J. Climate, 14, 4308–4318,
596   https://doi.org/10.1175/1520-457 0442(2001) 014,4308:IVOTRS.2.0.CO;2.

597   24. Mason, S. J. and N. E. Graham, (2002). Areas beneath the relative operating characteristics
598   (ROC) and relative operating levels (ROL) curves: statistical significance and

599   interpretation. Quar. Roy. Soc., 128, 2145-2166.
600   https://doi.org/10.1256/003590002320603584

601   25. Misra, V. (2004) An evaluation of the predictability of austral summer season precipitation
602   over South America. Journal of Climate, **17**, 1161–1175. https://doi.org/10.1175/1520-
603   0442(2004)017<1161:AEOTPO>2.0.CO;2

604   26. Misra, V., Dixit, S., & Jayasankar, C. B. (2023). The regional diagnosis of onset and demise
605   of the rainy season over tropical and subtropical Australia. Earth Interactions, 27(1),
606   220026. https://doi.org/10.1175/EI-D-22-0026.1

607   27. Misra, V., Jayasankar, C. B., Beasley, P., & Bhardwaj, A. (2022). Operational monitoring
608   of the evolution of rainy season over florida. Frontiers in Climate, 4, 793959.
609   https://doi.org/10.3389/fclim.2022.793959

610   28. Misra, V.; Bhardwaj, A.; Mishra, A. (2018). Local onset and demise of the Indian summer
611   monsoon. Clim. Dyn., 51, 1609–1622. https://doi.org/10.1007/s00382-017-3924-2

612   29. Misra, V.; Bhardwaj, A.; Noska, R. (2017) Understanding the Variations of the Length and
613   the Seasonal Rainfall Anomalies of the Indian Summer Monsoon. J. Clim., 30, 1753–1763.
614   https://doi.org/10.1175/JCLI-D-16-0501.1

615   30. Misra V, DiNapoli S (2014) The variability of the southeast Asian summer monsoon. Int J
616   Climatol 34:893–901. https://doi.org/10.1002/joc.3735

617   31. Mitra, A. K., Bohra, A. K., Rajeevan, M. N., & Krishnamurti, T. N. (2009). Daily Indian
618   precipitation analysis formed from a merge of rain-gauge data with the TRMM TMPA
619   satellite-derived rainfall estimates. 87A, 265-279. https://doi.org/10.2151/jmsj.87A.265

620   32. Mooley, D. A., and B. Parthasarthy (1984), Fluctuations in all-India summer monsoon
621   rainfall during 1871–1978, Clim. Change, 6(3), 287–301, doi:10.1007/BF00142477.
622   https://doi.org/10.1007/BF00142477

623   33. Mooley, D. A., and J. Shukla (1987), Variability and forecasting of the summer monsoon
624   rainfall over India, in Monsoon Meteorology, edited by C. P. Chang and T. N. Krishnamurti,
625   pp. 26–59, Oxford Univ. Press, Oxford, U. K

626   34. Moron V, Robertson AW, (2014): Interannual variability of Indian summer monsoon
627   rainfall onset date at local scale. Int J Climatol, 34(4). doi:10.1002/joc.3745

628   35. Noska, R.; Misra, V. (2016) Characterizing the onset and demise of the Indian summer
629   monsoon. Geophys. Res. Lett., 43, 4547–4554. https://doi.org/10.1002/2016GL068409

630   36. Pai DS, Rajeevan M (2007) Indian Summer Monsoon Onset: variability and prediction.
631   NCC Research Report No. 6. National Climate Centre, Indian Meteorological Department.

632   37. Pai, D. S., & Rajeevan, M. N. (2009). Summer monsoon onset over Kerala: New definition
633   and prediction. Journal of Earth System Science, 118(2), 123-135.
634   https://doi.org/10.1007/s12040-009-0020-y

635   38. Pai, D. S., Rajeevan, M., Sreejith, O. P., Mukhopadhyay, B., & Satbha, N. S. (2014).
636   Development of a new high spatial resolution (0.25× 0.25) long period (1901-2010) daily
637   gridded rainfall data set over India and its comparison with existing data sets over the
638   region. Mausam, 65(1), 1-18. https://doi.org/10.54302/mausam.v65i1.851

639   39. Pai, D. S., Bandgar Arti, Devi Sunitha, Musale Madhuri, M. R. Badwaik, A. P. Kundale,
640   Gadgil Sulochana, M. Mohapatra, and M. Rajeevan. (2020) "Normal dates of
641   onset/progress and withdrawal of southwest monsoon over India." Mausam 71, no. 4, 553-
642   570. https://doi.org/10.54302/mausam.v71i4.33

643   40. Phadtare, J. A., Fletcher, J. K., Ross, A. N., Turner, A. G., Schiemann, R. K., & Burns, H.
644   L. (2023). Unravelling the mechanism of summer monsoon rainfall modes over the west
645   coast of India using model simulations. Quarterly Journal of the Royal Meteorological
646   Society, 149(757), 3164-3182. https://doi.org/10.1002/qj.4550

647   41. Pradhan, M., Rao, A. S., Srivastava, A., Dakate, A., Salunke, K., & Shameera, K. S. (2017).
648   Prediction of Indian summer-monsoon onset variability: A season in advance. Scientific
649   reports, 7(1), 14229. https://doi.org/10.1038/s41598-017-12594-y

650   42. Prasad, V. S. & Hayashi, T. Onset and withdrawal of Indian summer monsoon. Geophys.
651   Res. Lett. **32**, 1–5 (2005). https://doi.org/10.1029/2005GL023269

652   43. Preenu, P. N., Joseph, P. V., & Dineshkumar, P. K. (2017). Variability of the date of
653   monsoon onset over Kerala (India) of the period 1870–2014 and its relation to sea surface
654   temperature. Journal of Earth System Science, 126, 1-19. https://doi.org/10.1007/s12040-
655   017-0852-9

656   44. Rajeevan, M. and Dubey, D. P., (1995) Long range prediction of monsoon onset over
657   Kerala, Mausam, V46, pp287-290. https://doi.org/10.54302/mausam.v46i3.3261

658   45. Ramage, C. (1971), Monsoon Meteorology, Int. Geophys. Ser., vol. 15, 296 pp., Academic
659   Press, San Diego, Calif.

660   46. Ramesh Kumar, M. R., (2004) Forecasting of onset of southwest monsoon over Kerala
661   coast using satellite data, IEEE Geosci. Remote Sens. Lett., V1 (4), pp265-267.
662   10.1109/LGRS.2004.832226

663   47. Rao, Y. P. (1976) Southwest monsoon. Meteorological Monograph, Synoptic Meteorology,
664   367.

665   48. Rodgers, J., Misra, V., & Jayasankar, C. B. (2024). Using the observed variations of the
666   start date of the rainy season over Central America for its reliable seasonal outlook. Journal
667   of Climate. *37*(18), 4901–4913. https://doi.org/10.1175/JCLI-D-23-0699.1

668   49. Saikrishna, T. S., Ramu, D. A., & Osuri, K. K. (2021). Inter-comparison of high-resolution
669   satellite precipitation products over India during the summer monsoon
670   season. Meteorology and Atmospheric Physics, 133, 1675-1690.
671   https://doi.org/10.1007/s00703-021-00829-7

672   50. Sankar, S., Kumar, M. R., & Reason, C. (2011). On the relative roles of El Nino and Indian
673   Ocean Dipole events on the Monsoon Onset over Kerala. Theoretical and applied
674   climatology, 103, 359-374. https://doi.org/10.1007/s00704-010-0306-7

675   51. Sperber, K. R., and H. Annamalai, (2014) The use of fractional accumulated precipitation
676   for the evaluation of the annual cycle of monsoons. Climate Dyn., 43, 3219–3244,
677   doi:10.1007/s00382-014-2099-3.

678   52. Stolbova, V., Surovyatkina, E., Bookhagen, B., & Kurths, J. (2016). Tipping elements of
679   the Indian monsoon: Prediction of onset and withdrawal. Geophysical Research Letters,
680   43(8), 3982-3990. https://doi.org/10.1002/2016GL068392

681   53. Thakur, M. K., Kumar, T. L., Narayanan, M. S., Kundeti, K. R., & Barbosa, H. (2020).
682   Analytical study of the performance of the IMERG over the Indian
683   landmass. Meteorological Applications, 27(3), e1908. https://doi.org/10.1002/met.1908

684   54. Walker, J. M., & Bordoni, S. (2016). Onset and withdrawal of the large-scale South Asian
685   monsoon: A dynamical definition using change point detection. Geophysical Research
686   Letters, 43(22), 11-815. https://doi.org/10.1002/2016GL071026

687   55. Wang B, Ding Q, Joseph PV (2009) Objective definition of the Indian summer monsoon
688   onset. J Clim 22(12):3303–3316. https://doi.org/10.1175/2008JCLI2675.1

689   56. Wang B, LinHo (2002) Rainy season of the Asia-Pacific summer monsoon. J Climate
690   15:386–398. https://doi.org/10.1175/1520-0442(2002)015<0386:RSOTAP>2.0.CO;2

57. Wang, X., Jiang, X., Yang, S., & Li, Y. (2013). Different impacts of the two types of El Niño on Asian summer monsoon onset. Environmental Research Letters, 8(4), 575–591. DOI 10.1088/1748-9326/8/4/044053

58. Webster, P. J., V. O. Magana, T. N. Palmer, J. Shukla, R. A. Tomas, M. Yanai, and T. Yasunari, (1998) Monsoons: Processes, predictability, and the prospects for prediction. *J. Geophys. Res.*, **103 ,** 14451–14510. https://doi.org/10.1029/97JC02719

59. Xavier, P. K., C. Marzin, and B. N. Goswami, 2007: An objective definition of the Indian summer monsoon season and a new perspective on the ENSO–monsoon relationship. Quart. J. Roy. Meteor. Soc., 133, 749–764, doi:10.1002/qj.45.

60. Xie, P., A. Yatagai, M. Chen, T. Hayasaka, Y. Fukushima, C. Liu, and S. Yang (2007), A gauge-based analysis of daily precipitation over East Asia, J. Hydrometeorol., 8, 607. 626. https://doi.org/10.1175/JHM583.1

61. Zeng X, Lu E (2004) Globally unified monsoon onset and retreat indexes. J Climate 17:2241–2248. https://doi.org/10.1175/1520-0442(2004)017<2241:GUMOAR>2.0.CO;2